

LOW-FLOW LIMIT IN SLOT COATING PROCESS OF BOGER LIQUIDS

Oldrich Joel Romero

PUC-Rio, Department of Mechanical Engineering
Rua Marquês de São Vicente, 225, 22453-900 – Rio de Janeiro, RJ, Brazil.
oldrich@mec.puc-rio.br

Márcio da Silveira Carvalho

PUC-Rio, Department of Mechanical Engineering
Rua Marquês de São Vicente, 225, 22453-900 – Rio de Janeiro, RJ, Brazil.
msc@mec.puc-rio.br

Abstract. Slot coating is a common method in the manufacture of a wide variety of products. The thickness of the coated liquid layer is set by the flow rate fed to the coating die and the speed of the substrate, and is independent of other process variables. An important operating limit of slot coating is the minimum thickness that can be coated at a given substrate speed, generally referred to as the low-flow limit. For Newtonian liquids, the mechanism that defines this limit balances the viscous, capillary and inertial forces in the flow. Although most of the liquids coated industrially are polymeric solutions and dispersions that are not Newtonian, most of the previous analyses of operability limits in slot coating dealt only with Newtonian liquids. In the case of liquids made non-Newtonian by polymer viscoelasticity, stresses can alter the force balance in various parts of the coating bead and consequently the onset of instability. In this work the low-flow limit of viscoelastic liquids is analyzed by theory. Two constitutive differential models, the Oldroyd-B and FENE-CR, are used to describe the viscoelastic behavior of dilute polymer solutions that present constant shear viscosity and extensional thickening viscosity, the so called Boger fluid. These differential models coupled with the conservation equations of mass and momentum are used to describe the flow in a slot coating process, considered in our work as two-dimensional, isothermal, incompressible and in steady state. The mixed, elliptic-hyperbolic, behavior of the system of equations is treated with the DEVSS-TG (Discrete Elastic-Viscous Split Stress, independent Traceless velocity Gradient interpolation) technique of Guenette & Fortin (1995), Sun et al. (1999) and Pasquali & Scriven (2002). The conservation equations are solved with the Galerkin/Finite Element Method and the constitutive differential equations with the Petrov-Galerkin/Finite Element Method. The results show how viscoelastic behavior of the flowing liquid alters the stress field near the free surface and consequently the low-flow limit of the process.

Keywords. Slot coating process, low-flow limit, finite element method, free surface, viscoelasticity.

1. Introduction

Slot coating is commonly used in the manufacturing of many different products. The coating liquid is pumped to a coating die, is distributed across the width of a narrow slot in a distribution chamber and, as it exits the slot, the liquid fills the gap between the die and the moving substrate. The liquid in the gap, bounded upstream and downstream by gas-liquid interfaces, or menisci, forms the coating bead, as shown in Fig. 1. The competition among viscous, capillary and pressure forces, and in some cases inertial and elastic forces, sets the range of operating parameters in which the viscous free surface flow of the liquid can be two-dimensional and steady. The region in the operating parameters of a coating process where the delivered liquid layer is adequately uniform is usually referred to as coating window. Knowledge of coating windows of different coating methods is needed in order to predict whether a particular method can be used to coat a given substrate at a prescribed production rate.

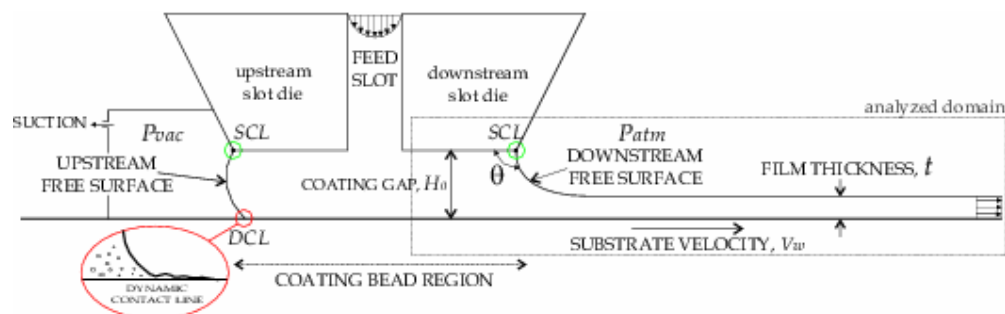


Figure 1: Sketch of slot coating bead. The analyzed domain is the downstream section of the bead.

Romero et al. (2004) reviews the different analyses of slot coating flows and predictions of the coating window of the process for both Newtonian and non Newtonian liquids. The main contributions for Newtonian flows are by Ruschak (1976), Higgins and Scriven (1980), Sartor (1990), Gates and Scriven (1996) and Carvalho and Kheshgi (2000). They show that for low viscosity liquids, the most important limit in slot coating process occurs when, at a given substrate speed, too low a flow rate per unit width from the slot causes the downstream meniscus to curve so much that it cannot bridge the gap's clearance H_0 . Consequently the meniscus becomes progressively more three-dimensional, alternate parts of it invading the gap until the bead takes a form that delivers separate rivulets or chains of droplets to the substrate moving past. This transition from a continuous coated liquid layer is what is called here the low-flow limit: the minimum thickness of liquid that can be deposited from a gap of specified clearance at a given substrate speed. It is independent of the vacuum applied, given that the vacuum is great enough to draw the upstream meniscus away from the feed slot. The coating window of the process when the low-flow limit is the principal mechanism of failure is sketched in Fig. 2.

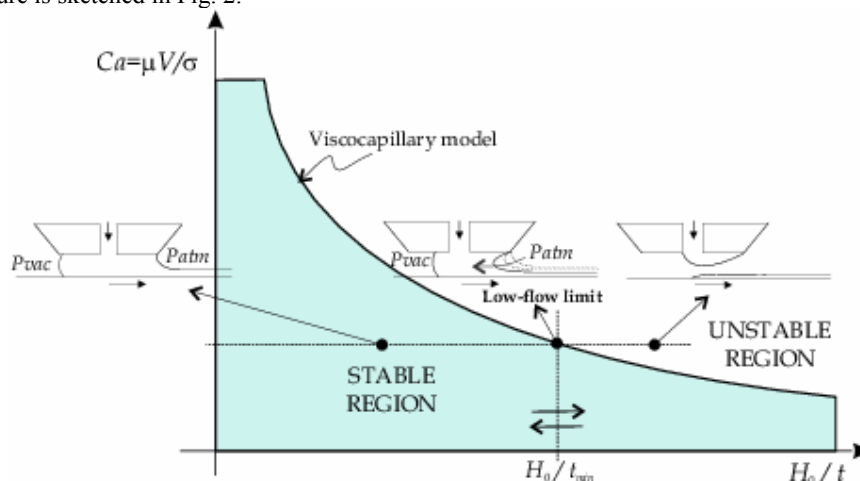


Figure 2: Critical conditions at the onset of low flow limit in slot coating process.

Liquids coated in practice are polymer solutions or colloidal suspensions, or both. In general, polymer solutions may be shear-thinning, extension-thickening, and develop viscoelastic stresses when sheared or extended. These liquids can depart substantially from Newtonian behavior at the strain rates they suffer in the coating flow. Ning et al. (1996) studied experimentally the effect of polymer additives on slot coating. However, they used no vacuum (reduced pressure) on the upstream meniscus and so the coatability limit they measured is not, as claimed, the low-flow limit of the process. Dontula (1999) analyzed experimentally the flow of polymer solutions in several coating processes. Model aqueous solutions with nearly constant viscosity and adjustable elasticity were developed to study the role of elasticity in coating and other free surface flows. The experiments showed that the free surface flow in the coating bead can be drastically changed even when only minute amounts of the high molecular polymers were added to the coating liquid. High molecular weight polymers that modify the mechanical behavior of coating solutions has been used to enlarge the coating window of slot coating of adhesives. Northey (1997) presented a water-based pressure sensitive adhesive formulation with one or more high molecular weight linear aliphatic polymer that made possible slot coating the liquid at a flow rate substantially less than the minimum delivery flow rate achievable using a coating formulation without polymer.

Romero et al. (2004) examined the low-flow limit in slot coating of aqueous solutions of low molecular weight PEG and high molecular weight PEO by both experiments and theory. A benchtop slot coating apparatus was used to visualize the coating bead at different operating conditions and observe the breakup mechanism. The experiments showed that, at a fixed capillary number, as the concentration of PEO rises and consequently the as the liquid becomes more viscoelastic, the minimum coated thickness possible increases. The operating window of the process is smaller when liquids with high extensional viscosity are used. The theoretical analysis consisted of solving the momentum and continuity equation system for steady, two-dimensional, free surface flow including a Generalized Newtonian model to describe the liquid rheological behavior. The constitutive equation used relates the stress to the rate-of-strain and relative-rate-of-rotation tensors. Such class of models is perhaps the simplest one that may capture the different ways that polymer molecules behave in extension-dominated and shear-dominated flow regions, but it is not able to describe viscoelastic stresses per se. The results obtained with the simple algebraic model agreed qualitatively with the experimental observations of low concentration polymer solutions, which presented high extensional viscosity and no measurable viscoelastic stresses.

In this work, the low-flow limit of slot coating of mildly viscoelastic liquids, that can be represented by Boger liquids, is examined by solving the conservation of momentum and continuity equations for steady, two-dimensional

flow with free surfaces, coupled with differential constitutive models that describe the mechanical behavior of dilute polymer solutions. Two models were tested, the Oldroyd-B and the FENE-CR constitutive relations. The system of equations was solved by the Galerkin and Petrov-Galerkin / Finite Element Method. At each operating condition (liquid properties as well as coating gap and web speed), a sequence of states was found by Newton iterations initialized by first-order, pseudo-arc-length continuation, i.e. a solution path in parameter space was constructed as the flow rate delivered to the die was diminished. The theoretically determined low-flow limit was defined by the parameter values at which the angle between the downstream free surface and the downstream die lip became less than 10° , as done by Carvalho and Khesghi (2000) and Romero et al. (2004).

2. Mathematical Formulation

The flow in the coating bead was described by the complete two-dimensional, steady-state mass and momentum conservation equations for free surface flows coupled with two differential constitutive models to describe the mechanical behavior of the liquid. The flow domain where the governing equations are solved is restricted to the region close to the downstream free surface, as sketched in Fig.3. Carvalho and Khesghi (2000) have shown that the flow upstream the feed slot does not affect the critical conditions at which the low flow limit occurs.

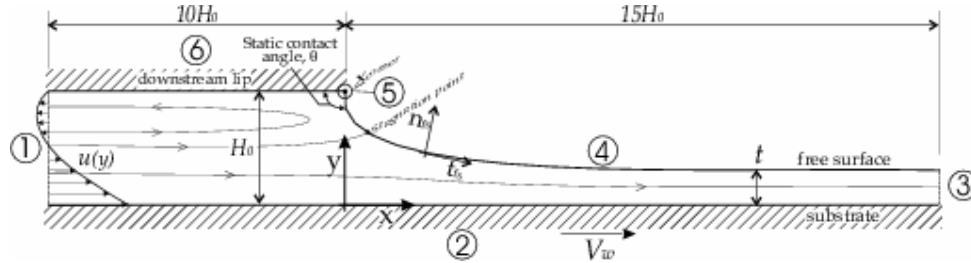


Figure 3: Domain at which the governing equations are integrated.

2.1. Governing Equations and Boundary Conditions

The velocity and pressure fields of two-dimensional Stokes flow are governed by the momentum and continuity equations:

$$-\nabla p + \nabla \cdot \boldsymbol{\tau} = 0, \quad \nabla \cdot \mathbf{v} = 0 \quad (1)$$

The extra-stress tensor $\boldsymbol{\tau}$ is the sum of the Newtonian solvent stress $\boldsymbol{\tau}_s$ and the polymeric stress $\boldsymbol{\tau}_p$. The constitutive models used here that relates the polymeric stress and the liquid deformation are presented in the following sub-section.

The no-slip and no-penetration conditions applies at the die wall (boundary 6 in Fig.3) and at the substrate (boundary 2). At the outflow plane (boundary 3), the directional derivative of velocity is set to zero.

At the free surfaces (boundary 4 in Fig.3), the traction in the liquid balances the capillary pressure and there is no mass flow across the gas-liquid interface:

$$\mathbf{n} \cdot \mathbf{T} = \frac{1}{Ca} \frac{dt}{ds} - \mathbf{n} P_0, \quad \mathbf{n} \cdot \mathbf{v} = 0. \quad (2)$$

\mathbf{t} and \mathbf{n} are the unit tangent and normal vectors to the interface, s is the arclength coordinate along the free surface and P_0 is the pressure of the air. At the downstream free surface, the air pressure is usually atmospheric, i.e. $P_0 = P_{ATM}$. The Capillary number $Ca = \mu V / \sigma$ measures the ratio between viscous and capillary forces (σ is the liquid surface tension).

At the inflow plane (boundary 1), the flow is assumed to be fully developed:

$$\mathbf{i} \cdot \mathbf{v} = 0; \quad \mathbf{j} \cdot \mathbf{v} = -\frac{6Q}{H_0} \left[\left(\frac{y}{H_0} \right) - \left(\frac{y}{H_0} \right)^2 \right]. \quad (3)$$

H_0 is the gap between the die and the substrate and Q is the flow rate fed into the coating die. It defines the thickness t of the liquid layer deposited onto the substrate: $t = Q/V$, where V is the web speed.

The static contact line attached to the downstream free surface (table 5 in Fig.3) is pinned at the sharp edge of the die, i.e. the position \mathbf{x}_{sd} of the downstream static contact line is fixed:

$$\mathbf{x}_{sd} = \mathbf{X}_{edge} \cdot \quad (4)$$

2.2. Constitutive Laws

Some aspects of dilute polymer solution flow can be captured by dumbbell models, which consist of describing the flexible polymer molecules by beads-and-springs chains. The stretching of the spring models the elastic forces of the polymer molecule, and the beads, the hydrodynamic drag forces of the solvent. The different forms of the evolution equation of the polymer conformation and the expression for the spring constant lead to different differential constitutive models. Here, in order to analyze the effect of viscoelastic forces of dilute polymer solutions in slot coating flows, two models - the Oldroyd-B and FENE-CR - were used. These models are adequate to represent the behavior of Boger type liquids, like the ones used by Dontula (1999) and Romero et al. (2004) in their experiments, that exhibit elastic stresses and constant shear viscosity.

In the Oldroyd-B model, the spring force (elastic) is a linear function of the polymer stretching. Therefore, each polymer molecule can be infinitely extended, leading to unbounded polymer stress in a purely extensional flow. In the FENE (Finite Extensible Nonlinear Elastic) models, the spring constant is a non-linear function of the polymer stretching. For small extension, the elastic spring force is linear, and a finite length is obtained in the limit of infinite force. With this non-linear spring function, the unbounded polymer stress in purely extensional flow predicted by the Oldroyd-B model is eliminated. The evolution equations of the polymer stress for the Oldroyd-B (eq.5) and FENE-CR (eq.6) models are:

$$\boldsymbol{\tau}_p + \lambda \boldsymbol{\tau}_{p(1)} = \eta_p \dot{\boldsymbol{\gamma}} \quad (5)$$

$$\boldsymbol{\tau}_p + \lambda \boldsymbol{\tau}_{p(1)} - \lambda \boldsymbol{\tau}_p \frac{D(\ln Z)}{Dt} = Z \eta_p \dot{\boldsymbol{\gamma}} \quad (6)$$

In both equations, $\boldsymbol{\tau}_{p(1)} \equiv \mathbf{v} \cdot \nabla \boldsymbol{\tau}_p - \nabla \mathbf{v}^T \cdot \boldsymbol{\tau}_p - \boldsymbol{\tau}_p \cdot \nabla \mathbf{v}$ is the upper convected derivative of the polymeric stress tensor. The parameter Z in the FENE-CR transport equation is defined as

$$Z \equiv \frac{1 + \left(\frac{\lambda}{b \eta_p} \right) tr(\boldsymbol{\tau}_p)}{1 - 3/b}$$

The rheological parameters are the relaxation time λ , the polymer viscosity η_p , and the dimensionless extensibility parameter b . As the later approaches infinity, the polymer molecules can be extended without bounds, Z approaches unity and the FENE-CR equation reduces to the Oldroyd-B model.

3. Solution Method

The differential equations that govern this situation are posed in an unknown domain; the position of the liquid free surface is part of the solution. A simple way of solving this type of problem is to use a Picard iteration, i.e. solve the flow and the domain position separately. This procedure is not very efficient and in most cases the iteration does not converge. To compute a free boundary problem, like this one, in a more efficient way, the set of differential equations posed in the unknown physical domain has to be transformed to an equivalent set defined in a known reference domain, usually called computational domain. This transformation is made by a mapping $\mathbf{x} = \mathbf{x}(\boldsymbol{\xi})$ that connects the two domains. The mapping used here is the one presented by de Santos (1991). He showed that a functional of weighted smoothness can be used successfully to construct the sorts of maps involved here. The inverse of the mapping that minimizes the functional is governed by a pair of elliptic differential equations identical with those encountered in diffusion transport with variable diffusion coefficients. The coordinates ξ and η of the reference domain satisfy

$$\nabla \cdot (D_\xi \nabla \xi) = 0; \quad \nabla \cdot (D_\eta \nabla \eta) = 0. \quad (7)$$

D_ξ and D_η are diffusion like coefficients that control the spacing between lines of constant ξ and η . Boundary conditions are needed in order to solve the second-order partial differential equations (7). Along solid walls and synthetic inlet and outlet plates, the boundary is located by imposing a relation between the coordinates x and y from the equation that describes the shape of the boundary and stretching functions are used to distribute the points along the

boundaries. The free boundaries (gas-liquid interfaces) are located by imposing the kinematic condition (eq.2-b). The discrete versions of the mapping equations are generally referred to as mesh generation equations.

Several different modifications to the transport equations that describe the flow of viscoelastic liquids have been proposed in recent years with the goal of stabilizing the numerical solution of the system. The formulation used here is the modification proposed by Pasquali and Scriven (2002) of the DAVSS (Discrete Adaptive Viscous Stress Split) formulation of Sun et al. (1999).

Each independent field, i.e. velocity, pressure, interpolated velocity gradient, polymeric stress tensor and the position of the nodal points, is approximated with a linear combination of a finite number of basis functions. The selection of the approximation spaces for the field variables hinges on the issues of compatibility conditions between the spaces for velocity and pressure, and velocity gradient and polymeric stress. The velocity and node position are represented in terms of bi-quadratic basis functions and the pressure with linear discontinuous functions. The interpolated velocity gradient and the polymeric stress are approximated with the same order polynomial, bi-linear basis functions.

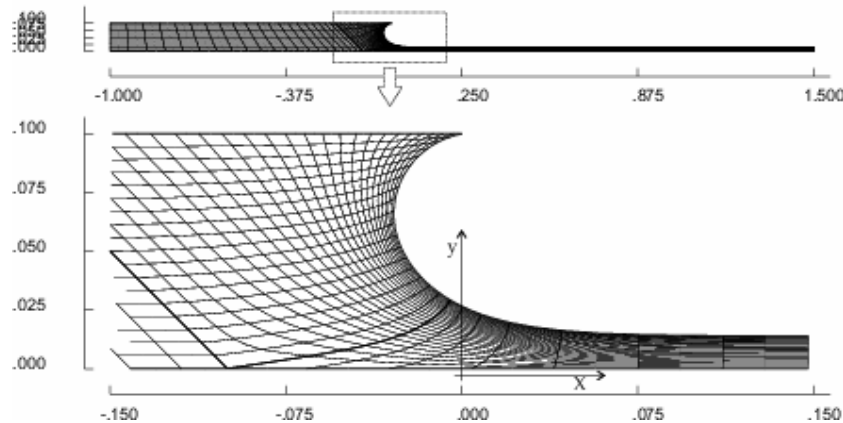


Figure 4: Detail of the mesh near the free surface.

The weighted residual equations are obtained after multiplying each governing equation by weighting functions, integrating over the unknown flow domain, applying the Gauss Theorem to the terms with second derivatives and mapping the integrals onto the known reference domain. Galerkin method is used in the residual equations of conservation of momentum, continuity, mapping and interpolated velocity gradient. Streamline upwind Petrov-Galerkin weighting functions are used in the hyperbolic constitutive equation.

Once all the variables are represented in terms of the basis functions, the system of partial differential equations reduces to simultaneous algebraic equations for the coefficients of the basis functions of all the fields. Because the basis function used are different from zero over a very small portion of the domain, the Jacobian matrix is sparse and stored in compressed sparse formats. This set of non-linear equations was solved by Newton's method with numerical jacobian. In each iteration the linearized equation system was factorized into unit lower **L** and unit upper **U** triangular matrix by a frontal solver. In order to improve the initial guess at each new set of operating conditions, a pseudo-arc-length continuation method, as described by Keller (1985), was used. The tolerance on the L2-norm of the residual vector and Newton's update was set to 10^{-6} . The domain was divided into 1810 elements, with approximately 49,000 unknowns. Figure 4 shows details of the mesh near the free surface.

4. Results

The operating conditions at which the low-flow limit occurs were determined theoretically by following a solution path constructed at a fixed capillary number and decreasing flow rate, as explained by Carvalho and Kheshgi (2000) and Romero et al. (2004). As the thickness of the deposited liquid film falls, the downstream free surface becomes more curved in order to create a larger adverse pressure gradient under the meniscus, and consequently the angle of the free surface with the die land diminishes. Romero et al. (2004) presented details of the Newtonian flow kinematics at different operating conditions. The low-flow limit was determined by searching for the value of gap-to-thickness ratio at which the static contact angle between the downstream free surface and the die lip reached $\theta = 10^\circ$. Using this approach, an operating window can be constructed, where the critical condition, e.g. gap-to-thickness, is graphed as a function of the capillary number. The predicted critical conditions for Newtonian liquids agree well with experimental observations.

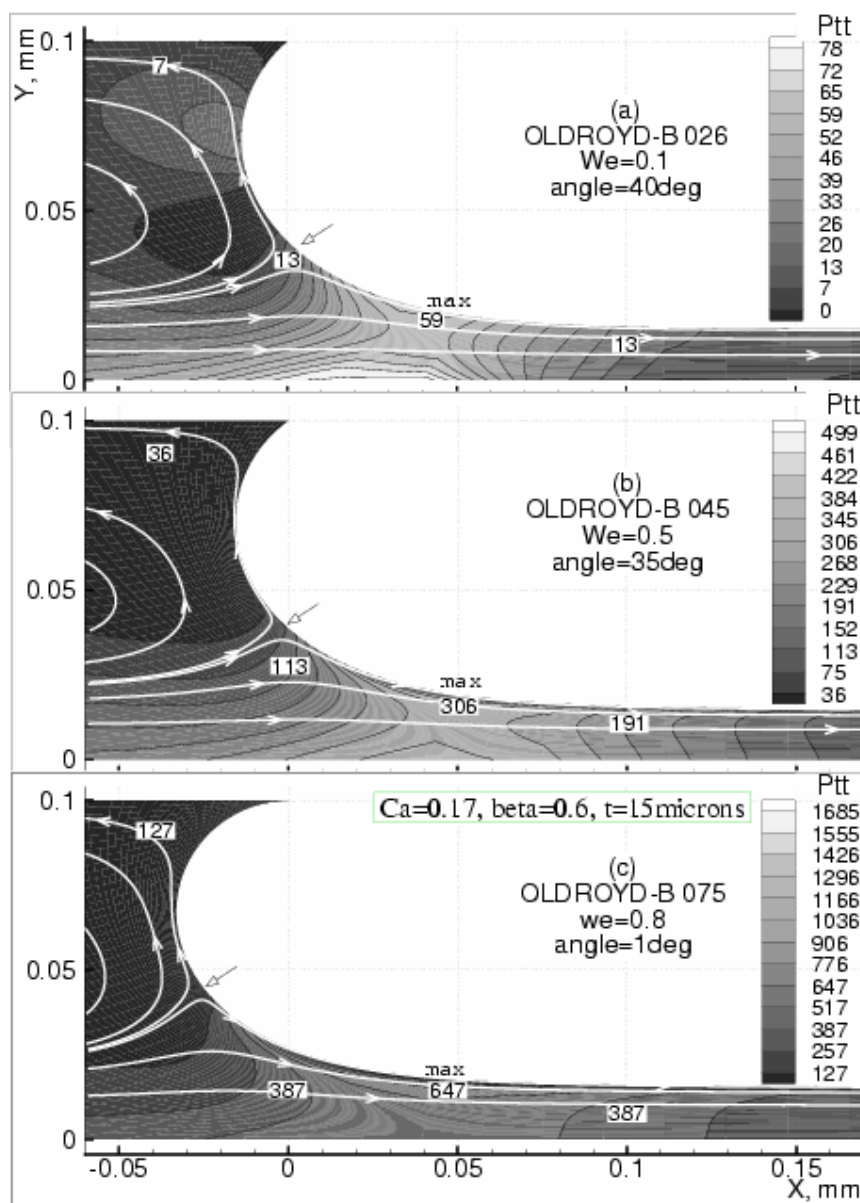


Figure 5: Polymeric normal stress component in the direction of the streamlines near the free surface as the Weissenberg number rises.

Viscoelastic forces near the downstream free surface changes the meniscus configuration of slot coating flows, as shown by the theoretical predictions of Pasquali and Scriven (2002) and Lee et al. (2002). Consequently, the minimum film thickness that can be coated at a given capillary number (substrate speed) is also affected by the viscoelastic behavior of the coating liquid, as observed in the experiments presented by Romero et al. (2004).

The evolution of the normal component of the polymeric stress along the streamlines and the meniscus configuration as the Weissenberg number rises at $Ca = 0.17$ and $H_0 / t = 5.9$ is shown in Fig.5. The viscoelastic behavior was described by the Oldroyd-B model and the ratio of the solvent viscosity to the total viscosity was $\beta = 0.6$. The stretching of the polymer molecules in the extension dominated flow near the free surface creates an elastic stress boundary layer attached to the meniscus as the liquid becomes more viscoelastic. In order to counter balance the action of the positive gradient of the polymeric stress along the free surface, which tends to push more liquid into the coated film, the free surface has to curve more to create a higher pressure gradient under the free surface and consequently the static contact angle of the free surface with the die land falls. The static contact angle as a function of gap-to-thickness ratio H_0 / t , at $Ca = 0.17$ and $Ca = 0.51$, and different Weissenberg numbers, predicted by the Oldroyd-B constitutive model, is presented in Fig.6. The Newtonian predictions are also shown for reference. When the angle between the free surface and the die land is large, e.g. $\theta > 100^\circ$, the deformation rates are relatively small and the effect of the

viscoelastic properties of the liquid is weak. At smaller contact angles, the free surface is more curved and the deformation rate near the free surface is much larger. In these cases, the viscoelastic forces are important and the contact angle becomes a strong function of the Weissenberg number. The results show that the effect of the liquid elasticity on the static contact angle and on the critical conditions at the onset of the low-flow limit is not monotonic. There is a small range of Weissenberg number at which the static contact angle rises as the liquid becomes more elastic (at a fixed capillary number and coated film thickness). At $Ca = 0.17$, the minimum film thickness that can be coated at $We = 0.1$ is smaller than the critical value obtained with Newtonian liquid. At larger values of Weissenberg numbers, the liquid viscoelasticity reduces the static contact angle, at a fixed capillary number and film thickness, and destabilizes the flow. Similar behavior can be observed at higher capillary number, e.g. $Ca = 0.51$, but the effect of the liquid elasticity is weaker. The main conclusion from these predictions is that although elastic forces tend to destabilize the flow, leading to larger minimum film thickness that can be coated at a given substrate speed, weak elastic forces (flow at small Weissenberg number) may stabilize the flow, leading to small minimum film thickness.

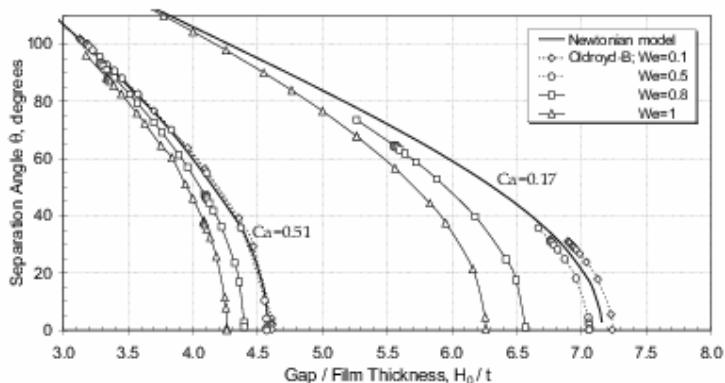


Figure 6: Angle between the downstream free surface and the die land as a function of gap-to-thickness ratio, capillary number and Weissenberg number.

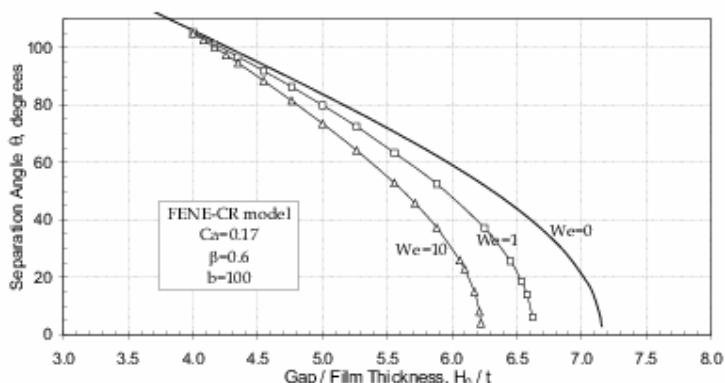


Figure 7: Effect of the Weissenberg number on the contact angle. Predictions obtained with the FENE-CR model.

The stress singularity associated with the Oldroyd-B model (linear dumbbell) does not allow the computation to proceed to higher Weissenberg numbers. To overcome this limitation, the viscoelastic behavior of the flowing liquid was also described by the FENE-CR model, which predicts a bounded extensional viscosity. The angle of the free surface with the die lip is presented in Fig.7 as a function of gap-to-thickness ratio and Weissenberg number, at capillary number $Ca = 0.17$, solvent-to-total viscosity ratio $\beta = 0.6$, and extensibility parameter $b = 100$. Solutions were obtained up to $We = 10$. The finite extensibility of the polymer molecules in the FENE-CR model makes the polymeric stress along the free surface smaller than those obtained with the Oldroyd-B model. Figure 8 presents the normal polymeric stress component tangent to the free surface as a function of the extensibility of the polymer molecules b . The elastic stress is small near the contact line, where there is a large recirculation. Downstream of the stagnation point on the free surface, the polymer molecules are extended and there is a high stress region. The maximum stress rises as the molecules become more flexible (higher b), as expected. The largest stresses are obtained with the Oldroyd-B model, which corresponds to an infinitely extensible molecule, i.e. $b = \infty$. The effect of the extensibility parameter on the static contact angle at $\beta = 0.6$, $We = 1$ and $Ca = 0.17$ is shown in Fig.9. The Newtonian liquid predictions are also shown as basis for comparison. The effect of the extensibility parameter b on the onset of the low-flow limit is not monotonic. At low extensibility parameter, e.g. $b = 20$, the liquid elasticity rises the contact angle

at a given capillary number and gap-to-thickness ratio, and the low-flow limit occurs at smaller film thickness, when compared to the Newtonian flow; the viscoelastic behavior of the coating liquid stabilizes the flow. At larger values of extensibility parameters, the liquid elasticity decreases the angle of the free surface with the die land and the low-flow limit occurs at thicker coating layer, when compared with the Newtonian flow; the viscoelastic behavior of the liquid destabilizes the flow.

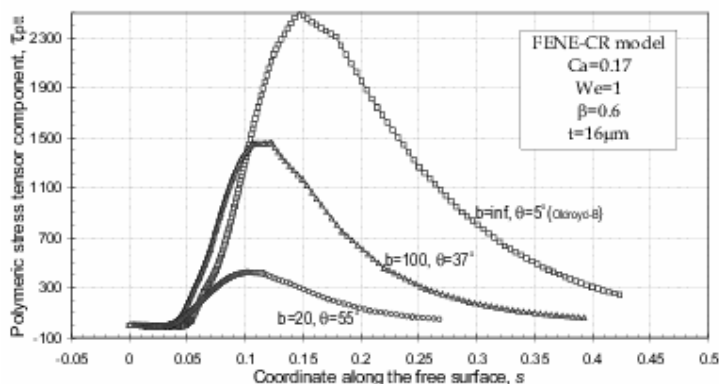


Figure 8: Polymeric stress tensor component along the free surface as a function of the extensibility parameter.

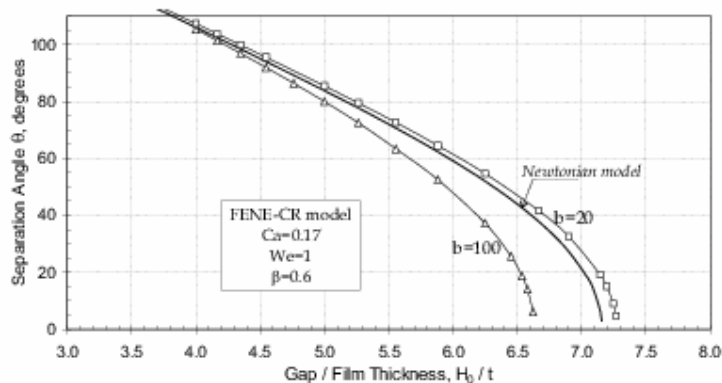


Figure 9: Effect of the finite extensibility parameter b on the contact angle.

The critical gap-to-film thickness ratio at different capillary numbers of slot coating process with viscoelastic liquids predicted by the Oldroyd-B model is presented in Fig.10. The results follow the same trends as the experiments reported by Romero et al. (2004), i.e. the larger relaxation time of the liquid (Weissenberg number) the thicker is the coated layer at the onset of the low flow limit. The process window is narrower when viscoelastic liquids are used. The effect of the elastic properties on the onset of the low-flow limit is more pronounced at lower capillary numbers. The critical conditions at $Ca = 0.17$ for both the Oldroyd-B and FENE-CR at different rheological parameters are summarized in Table 1. The results with both models show that when the elastic forces are weak, i.e. low Weissenberg number or low finite extensible parameter b , the liquid elasticity stabilizes the flow, leading to thinner coated layer; and when the elastic forces are strong, the liquid elasticity destabilizes the flow, leading to larger minimum coating thickness. This non-monothonic behavior was not observed in the experiments of Romero et al. (2004), but agrees with the behavior reported by Northey (1997): the addition of small quantities of high molecular weight polymer stabilize the process, that in their analysis was represented by smaller flow rate at a fixed substrate speed.

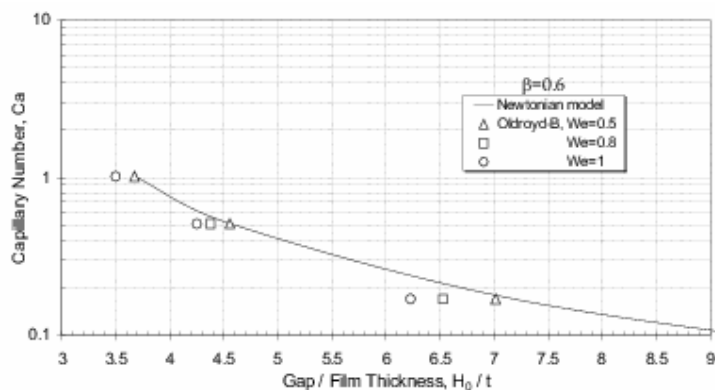


Figure 10: Critical conditions at the onset of the low flow limit. Predictions with the Oldroyd-B model.

Table 1: Effect of the rheological properties and constitutive model on the critical conditions at onset of the low flow limit at $Ca = 0.17$.

Constitutive Model	We	β	b	H_0/t
NEWTONIAN	0.0	1.0		7.18
OLDROYD-B	0.1	0.6	∞	7.25
	0.5		∞	7.01
	0.8		∞	6.52
	1.0		∞	6.24
FENE-CR	1.0	0.6	20	7.26
			100	6.6

5. Final Remarks

Slot coating is one of the preferred methods for high precision coating. There is an important operating limit, known as the low-flow limit, when thin films of low to medium viscosity liquids are coated at relatively high speeds. It is caused by the receding action of the downstream free surface as the flow rate is reduced at a fixed substrate speed. The operating parameters at which the coating bead breaks has been determined by previous researchers in the case of Newtonian liquids. However, most of the liquids coated industrially are polymeric solutions and dispersions, which are non-Newtonian. In general, polymer solutions may be shear-thinning, extension-thickening, and develop viscoelastic stresses when sheared or extended. These liquids can behave dramatically differently from Newtonian liquids in coating flows. Romero et al. (2004) used a benchtop slot coating apparatus to visualize the coating bead at different operating conditions and observe the breakup mechanism when viscoelastic liquids (Boger liquids) are used. The experiments showed that, at a fixed capillary number, as the concentration of the high molecular weight polymer rises and consequently as the liquid becomes more viscoelastic, the minimum coated thickness possible increases. The operating window of the process is smaller when liquids with high extensional viscosity are used. On the other hand, Northey (1997) have shown examples where the addition of high molecular weight polymer made possible slot coating adhesive formulation at a flow rate substantially less than the minimum flow rate achievable using a coating formulation without polymer.

This work presented a theoretical analysis of slot coating viscoelastic liquids that consisted of solving the momentum and continuity equation system for steady, two-dimensional, free surface flow coupled with differential constitutive models (Oldroyd-B and FENE-CR) to describe the rheological behavior of dilute polymer solutions. The free boundary problem was solved by mapping the unknown physical domain to a fixed reference domain. The full set of differential equations, including the transformation mapping from the physical to the reference domain, was solved all together by the finite element method. The theoretical low-flow limit was defined by the parameters at which the static contact angle between the downstream free surface and the die lip became less than 10° .

The results confirm the experimental observations reported in the literature. If the viscoelastic stresses are small, i.e. low Weissenberg number and less flexible polymer molecules, the onset of the low flow limit occurs at lower flow

rate than the Newtonian case, i.e. the viscoelasticity stabilizes the process and leads to a wider coating window. Above a certain value, the viscoelastic stresses destabilizes the process, leading to narrower process windows.

6. Acknowledgement

The authors would like to thank Prof. Matteo Pasquali for discussions on viscoelastic flow modelling during his stay at PUC-Rio.

This work was partially funded by CNPq and FAPERJ.

7. References

- Beguín, A. E., 1954, "Method of Coating Strip Material". U.S. Pat. 2,681,294.
- Brooks, A. N. and Hughes, T. J. R., 1982, "Streamline upwind / Petrov-Galerkin formulations for convection dominated flows with particular emphasis on the incompressible Navier-Stokes equations", *Comput. Methods Appl. Mech. Eng.*, vol.32, pp.199-259.
- Bolstad, J. H. and Keller, H. B., 1985, "A multigrid continuation method for elliptic problems with folds", *SIAM Journal of Science Stat. Comput.*, vol.7, pp.1081-1104.
- Carvalho, M. S. and Keshghi, H., 2000, "Low Flow Limit in Slot Coating: Theory and Experiments", *AIChE Journal*, vol. 46(10), pp.1907-1917.
- De Santos, J. M., 1991, "Two-phase cocurrent downflow through constricted passages", Ph.D. Thesis, University of Minnesota.
- Dontula, P., Macosko, C.W. and Scriven, L.E., 1998, "Model elastic liquids with water-solvent polymers", *AIChE Journal*, vol.44(6), pp.1247-1255.
- Guenette, R and Fortin, M., 1995, "A new mixed finite element for computing viscoelastic flows", *Journal of Non-Newtonian Fluid Mechanics*, vol. 60, pp.27-52.
- Gates, I. D., 1996, "Stability Analysis of Slot Coating Flows". Presented at *AIChE 1996 Spring National Meeting*. New Orleans.
- Higgins, B. G. and Scriven, L. E., 1980, "Capillary pressure and viscous pressure drop set bounds on coating bead operability". *Chem. Eng. Sci.* vol.35, pp.673-682.
- Kistler, S. F. and Scriven, L. E., 1983, "Coating Flows", in J. R. A. Pearson and S. M. Richardson (eds), *Computational Analysis of Polymer Processing*, Applied Science Publishers, London, p.243.
- Lee, K. Y. and Liu, T. J., 1992, "Minimum web thickness in extrusion slot coating", *Chemical Engineering Science*, vol.47, pp.1703-1713.
- Lee, A. G., Shaqfeh, E. S. G. and Khomami, B., 2002, "A study of viscoelastic free surface flows by the finite element method: Hele-Shaw and Slot Coating Flows", *Journal of Non-Newtonian Fluid Mechanics*, vol.108, pp.327-362.
- Northey, P. J., 1997, "Coating Additives for Water-Based Formulations", U.S.Pat. 5,643,992.
- Pasquali, M. and Scriven, L. E., 2002, "Free surface flows of polymer solutions with models based on the conformation tensor", *Journal of Non-Newtonian Fluid Mechanics*, vol.108, pp.363-400.
- Romero, O. J., Suszynski, W. J., Scriven, L. E. and Carvalho, M. S., 2004, "Low flow limit in slot coating of dilute solutions of high molecular weight polymer", *Journal of Non-Newtonian Fluid Mechanics*, vol.118, pp.137-156.
- Ruschak, K. J., 1976, "Limiting flow in a pre-metered coating device". *Chem. Eng. Sci.* **31**, pp.1057-1060.
- Sartor, L., 1990, "Slot coating: Fluid mechanics and die design". PhD Thesis. University of Minnesota.
- Sun, J., Smith, M. D., Armstrong, R. C. and Brown, R. A., 1999, "Finite element method for viscoelastic flows based on the discrete adaptive viscoelastic stress splitting and the discontinuous Galerkin method: DAVSS-G/DG", *Journal of Non-Newtonian Fluid Mechanics*, vol.86, pp.281-307.